JOURNAL OF SOLID STATE CHEMISTRY **105**, 339–348 (1993)

Preparation and Characterization by AES of Niobium Diselenide Single Crystals

A. ROLLAND,* G. VACQUIER,† AND A. CASALOT†,‡

**Laboratoire de Métallurgie, U.A. 443, Faculté des Sciences et Techniques de St-Jérôme, Avenue Normandie-Niémen, 13397 Marseille Cedex 13, France; and †Laboratoire de Physico-Chimie des Matériaux, Université de Provence, Centre St-Charles, 3, place Victor-Hugo, 13331 Marseille Cedex 3, France*

Received April 20, 1992; in revised form December 10, 1992; accepted December 11, 1992

Niobium diselenide powder, $NbSe_2$, was prepared by direct synthesis from pure elements. Single crystals were obtained by chemical vapor transport (CVT) using iodine as a gas vector in a *three-zone* thermal profile and analyzed by Auger electron spectroscopy (AES). The bulk composition of deep-seated cleaved single crystals corresponds to the stoichiometric composition given by the $NbSe_2$ formula. The crystal surface is strongly reactive: superficial carbon adsorption occurs even in an ultravacuum atmosphere. In ambient air a thick superficial altered film is formed: the surface is oxide-coated and nitrogen is dissolved between the layers. Under iodine atmosphere, a simultaneous superficial adsorption of iodine, nitrogen, and carbon is observed, but the superficial layers are easily removed by argon sputtering. © 1993 Academic Press, Inc.

I. Introduction

The lamellar character of transition dichalcogenides favors the existence of several polytypes derived from the CdI_2-type structure due to variable stacking of MX_2 layers; iono–covalent bonds within the layers are revealed to be much stronger than molecular bonds between layers (*1*). Consequently, there is a marked anisotropy of physical properties normal to or parallel to the plane of the layers. The variable number of *d* electrons, not involved in chemical bonds, explains why some compounds, belonging to the VA transition group, such as $NbSe_2$ or 1T-TaS_2, are metallic at room temperature while others, including those of the IVA and VIA groups, such as ZrS_2 or $MoSe_2$, are insulators (*2*).

The lamellar structures of these materials permit the insertion between the layers of some organic molecules, such as pyridine (*3*), and even of some metals, such as alkali metals, as in the Na_xNbSe_2 phase (*4*). For some years, interest in these materials has focused on their transport properties (*5*) and, more particularly, on their use in energy photoconversion. Following the work of Tributsch (*6*), these materials act as semiconducting electrodes for photovoltaic effect recovery, the best of them being those with a gap value close to the 1.5 eV area (*7–9*).

Unfortunately, as major experimentation difficulties limit the production of large single crystals and thus their analysis, existing studies concern mostly polycrystalline materials or powders (*10*). A previous study by Auger spectroscopy, pointing out the surface reactivity of $NbSe_2$ single crystals (*11*), led us to search for the conditions of their synthesis. The aim of this paper is to present an experimental growth process for $NbSe_2$ single crystals and to characterize them by Auger electron spectroscopy (AES) in the hope of being able to extend the con-

---

‡ To whom correspondence should be addressed.

0022-4596/93 $5.00

clusions obtained to the production of other dichalcogenides (*12, 13*).

II. Experimental Procedures

2.1. Diselenide Powder Synthesis

Niobium diselenide is directly synthesized from the elements in powder (3 *N* Koch–Light for niobium) or in granular forms (5 *N* Koch–Light for selenium), using silica glass tubes sealed under secondary vacuum. During synthesis, the temperature is increased stepwise to 875 K in 48 hr, in order to avoid any risk of explosion due to fast selenium vaporization. Then the system is kept at a constant temperature of 1050 K for 72 hr before air quenching.

After intimate milling, a new 96- to 120-hr annealing at 1050 K takes place, followed by a slow cooling. The polycrystalline product so obtained, which is of very bright color, has been verified by X-ray diffraction (XRD), and the measured parameters (a = 345 pm, c = 1254 pm) are consistent with the literature values (*14*) and correspond to the 2-H polytype.

2.2. Diselenide Single Crystal Growth

Closed tube chemical vapor transport (CVT) has been routinely used since the original work of Schäfer (*15*) to obtain single crystals of high melting point or compounds of high vapor pressure. In the case of transition metal dichalcogenides TX_2 (X = Se, Te), the most commonly used transport agents are halogens (*14*), with iodine being the easiest to use because of its solid nature at ambient temperature (*16–18*).

$NbSe_2$ CVT has been accomplished with iodine. The transport reaction occurs in sealed tubes (ϕ_{int} = 9 to 13 cm; L = 25 cm) made of transparent silica glass. These tubes are carefully outgreased, etched (HF, 10%), and dried before the charge is introduced. In each experiment, the amount of diselenide, in polycrystalline form, is about 0.8 to 1 g.

Iodine, because of its high hygroscopicity, has been weighted and introduced into the transport tubes in a dry box under argon atmosphere. After a few minutes of degassing, the part of the ampoule filled with transport agent is immersed into liquid nitrogen. After a secondary vacuum degassing (P ~ 0.1 Pa) lasting 6 to 8 hr, the ampoule is sealed.

$NbSe_2$ crystal growth has been realized using the forced flux method described by Omaly *et al.* (*19*) in a ground prototype of the Multizone furnace constructed for the French Space Agency (CNES) for use in microgravity crystal growth experiments (*20*). This tubular furnace is composed of *three isothermal zones,* each from 5 to 10 cm long, produced by metallic diffuser blocks. These are separately controlled by PID electronic regulator–programmators (Eurotherm), with a stability of ±0.5 K in the temperature range 900–1300 K in which they are used. These various zones correspond to:

—a *source zone* S, which is used as a supply for the powder to be carried;

—a *growth zone* G, where germination and nucleation take place; and

—a *pitch zone* P, where crystal growth can occur if the transport agent concentration is too high.

To eliminate parasitic nucleation centers from the growth zone, it is necessary to realize first a *reverse transport* toward the *source zone*. This is obtained by way of the three regulator–programmator set which allows, at the beginning of each experiments, a thermal profile with $T_S < T_G < T_P$, where T_S, T_G, and T_P are respectively the *source zone, growth zone,* and *pitch zone* temperatures. After 24 hr reverse transport, T_S and T_P are automatically modified to correspond to the chosen crystal growth thermal profile with $T_S > T_G > T_P$.

With the aim of understanding the mechanism of transport of niobium diselenide by iodine, two of us have undertaken the examination of the thermal behavior of all products able to exist in the vapor phase (*21*). We have shown that the upper NbI_n iodides are degraded when the temperature increases (NbI_5 as early as 550 K, NbI_4 from 700 K); NbI_3 alone is present at high temperature. Our complete thermodynamic and kinetic study of iodine $NbSe_2$ CVT has finally shown that the chemical growth process is well described by the reaction (*22*):

$$NbSe_{2(s)} + \tfrac{3}{2}I_{2(g)} = NbI_{3(g)} + Se_{2(g)}.$$

The best crystals are obtained at an iodine concentration close to 1.5 to 3 g · l^{-1} and temperature zones of T_S = 1100 K, T_G = 1000 K, and T_P = 980 K. This configuration makes it convenient to control the crystal growth since supersaturating conditions separate the hydrodynamic process (convection and/or diffusion) from the thermodynamic process (nucleation and growth) within the vapor phase (*19*).

The single crystals which are obtained are hexagonal plates approximately 5 × 5 mm^2 large and 0.05 to 0.2 mm thick. After the transport cell is opened, the samples are cleaned with acetone in order to eliminate excess iodine and then stocked in pillboxes.

Structural analysis of the crystals was performed with the rotating crystal method. An extra check was made by examining the crushed, powdered crystals, using a gas-proportional diffractometer with a monochromator set beyond the device.

The CdI_2 structure ($P6_3/mmc$) and related structures give a lamellar characterization, hence facilitating a cleaving perpendicular to **c** axis. The parameters determined by XRD in a Weissenberg camera are a = 345.1 pm, c = 1254.2 pm, leading to the 2-H polytype (two $NbSe_2$ cell patterns) (*17*). Due to the absence of any $NbSe_3$ phase, as pointed out by Meerschaut and Rouxel (*23*), within prepared polycrystalline samples and also according to the chemical quantitative analysis by air oxidation (Nb_2O_5 formation), we can be quite sure it is a stoichiometric single crystal.

2.3. AES Characterization

The niobium diselenide single crystals are set out in a conventional ultrahigh-vacuum (UHV) chamber (the base pressure is in the 10^{-8} Pa range) which is equipped with a Riber cylindrical mirror analyzer. Argon ions are used to sputter-clean the surface.

The experimental conditions are as follows: argon dynamic pressure, 5 mPa; ion energy, 1.5 keV; beam current, 3 μA; beam diameter, 3 mm. Under these conditions, the sputtering rate is about 6 nm·hr^{-1}, a value close to that measured previously (*24*). The Auger spectra are recorded in the differential mode, the primary energy and modulation amplitude being respectively 2 keV and 4 eV (*25*).

III. AES Superficial Characterization

Auger analysis of the samples enables us to obtain dual information concerning the first layers located near the surface (2 or 3 MX_2 layers) and the distribution of all elements as a function of sputtering time (i.e., a deep sample study). However, because of its high sensitivity, Auger spectroscopy is very often disturbed by systematic perturbation due to impurities (carbon and oxygen, for instance). Oxygen generally gives very little parasite noise in our apparatus. In contrast, trails of gaseous carbon are always present in a UHV chamber either as impurities inside the material itself (called *segregated carbon*) or as carbon monoxide arising from outside contamination (grease on the walls, in and out operations) and adsorbed on the clean surface (called *adsorbed carbon*). The adsorbed quantity is always lower than an atomic single layer, with the absorption kinetics depending on the surface reactivity (pollution can require 24 hr for metals, such as silver (*24*), but only 1 to 2 min for amorphous silicon).

3.1. Bulk Single Crystal Analysis

Studies were made on samples cleaved immediately before they were put into the UHV chamber. Thus, their surface composition corresponded to the bulk composition of the crystal. A typical Auger spectrum

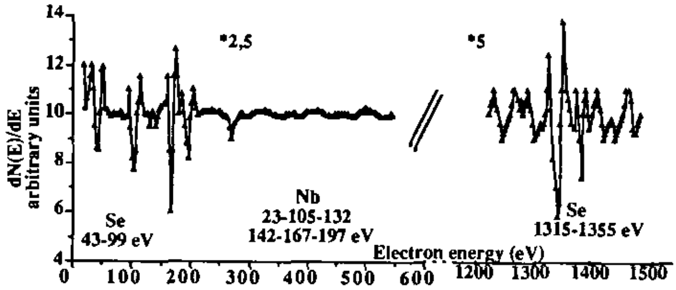

FIG. 1. AES spectrum of a $NbSe_2$ single crystal bulk.

is shown in Fig. 1. Auger signals of both elements are present (*26*): peaks at 23, 105, 132, 142, 167, and 197 eV for niobium; and peaks at 43, 99, 1315 and 1355 eV for selenium. This spectrum, which is quite similar to the one Mrstik *et al.* obtained by low-energy electron diffraction (LEED) (*27*), is completely independent of the sample conservation process.

A comparison between the ratio of peak-to-peak heights of both elements in the binary compound and those of the pure elements is a common method for quantitative Auger calibration (*28*). However, energies of Auger transitions must be very close, so that the escape depths of Auger electrons may be more or less the same.

The peak-to-peak ratio for low-energy transitions of selenium and niobium (respectively 43 and 23 eV) is about 2 for the compound when compared with the unit ratio deduced from the spectra of pure elements (*28*). For higher energies (respectively 1315 and 167 eV), this ratio is about 1.8. These ratios (particularly the low-energy one) are related to the superficial composition of a cleaved sample: the concentration of selenium is twice that of niobium. Thus, the single crystal bulk corresponds to the stoichiometric composition given by the $NbSe_2$ formula.

The single impurity detected on the surface of our cleaved samples corresponds to tiny carbon deposits. That element could be identified from a 272-eV peak, clearly visible also on the reference spectrum. A small quantity of carbon adsorbed on the surface is frequently observed in Auger spectrometry. Oxygen, iodine, and silica (basic material of the transport cell) are not seen in the depth of the sample, thus confirming the high purity of CVT single crystals.

This carbon pollution is far less important than that observed by Allie *et al.* (*29*) on $NbSe_2$ cleaved crystals prepared by the same method as ours (*30*). The carbon peaks they noted had such a high intensity that the niobium and selenium peaks were too low for any quantitative analysis.

Because under UHV the peak-to-peak ratio of carbon was twice as high after 24 hr, and because only a weak quantity of oxygen could be measured, we decided to undertake an extensive study of surface reactivity.

3.2. Superficial Layer Analysis

3.2.1. Recently made samples. An analysis of the superficial layers of a sample, set into a UHV cell a few hours after the transport tube was opened (under iodine conservation), has been conducted. The results are shown in Fig. 2.

The first spectrum (Fig. 2a) reveals superficial carbon and nitrogen pollution. Nevertheless, we must point out a double-range energy peak at 511 and 520 eV, which is a typical iodine doublet and different from oxygen whose spectrum has only one peak at 510 eV.

The intensity evolution of several peaks in the course of sputtering is represented in

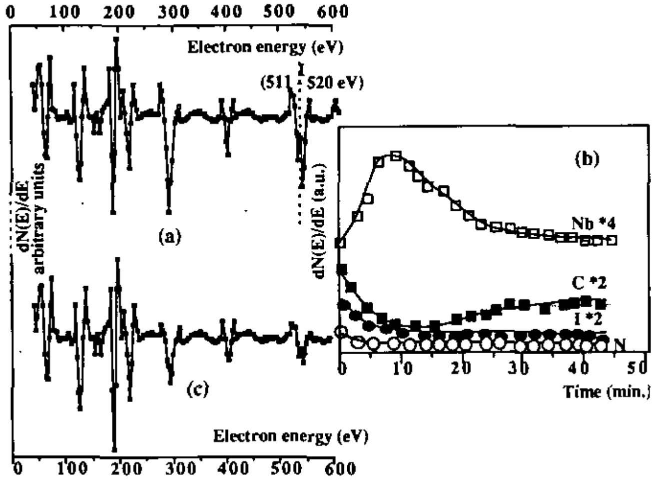

FIG. 2. Auger diffraction spectra of a $NbSe_2$ sample: (a) a few hours after transport cell opening; (b) evolution during a long ionic sputtering; (c) final result after ionic sputtering.

Fig. 2b. A clearly visible increase of the niobium peak can be noted (167 eV), meanwhile carbon, iodine, and nitrogen peaks rapidly become lower and disappear completely. The final spectrum is represented in Fig. 2c.

The time evolution of C, N, and I peaks shows that these elements have been superficially adsorbed. In contrast, the Nb peak lessening at $t > 5$ min can only be explained by the elaboration just after ionic sputtering of an altered layer (over several monoatomic layers) close to the surface: this can be linked to the physical property of anisotropy parallel or normal to the sample surface.

After 5 min of sputtering, the spectrum is similar to those obtained for cleaved single crystals. This means that iodine, for example, could be present in the bulk only at low concentrations, a result consistent with a neutron activation analysis made by Lewis *et al.* (*5*) in which they found 400–600 ppm of iodine in $NbSe_2$ single crystals obtained by CVT using iodide as a vector transport agent. A similar conclusion has already been obtained for $TiSe_2$ single crystals grown by the same method (*31*).

Auger analytic characterization of $NbSe_2$ single crystals obtained after chemical vapor transport thus shows the high range purity of bulk samples, but points out their strong surface reactivity, which is followed by the adsorption of various gases, and above all, their systematic pollution by carbon.

3.2.2. Deep ambient air contamination. The Auger spectrum of a $NbSe_2$ sample surface which had been left in ambient air for 3 months is represented in Fig. 3a. In addition to the Nb and Se peaks, we can see other high peaks, this time at 272 and 510 eV, and a weaker one, at 379 eV. They represent respectively carbon, oxygen, and nitrogen (*26*).

The evolution of Auger signals vs sputtering time is represented in Fig. 3b. There is a rapid decrease in the intensity of the carbon and selenium peaks, whereas the niobium, nitrogen, and oxygen peaks are increasing. After this, the intensity of all the signals remains steady whatever the sputtering duration. The final spectrum, after 8 hr of sputtering, is given in Fig. 3c.

For a short sputtering duration, the relative variations in the carbon, niobium, and oxygen signals indicate carbon adsorption on the surface, which leads to an extinction of niobium and oxygen Auger signals.

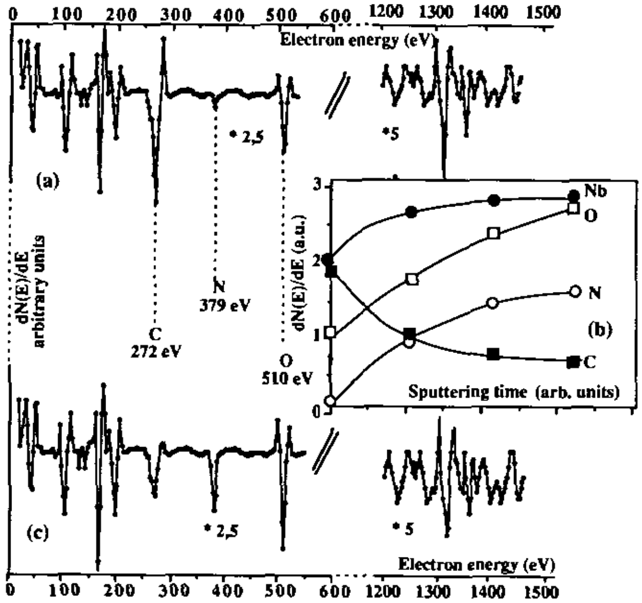

FIG. 3. Auger diffraction spectra of a $NbSe_2$ surface sample: (a) left in ambient air for 3 months; (b) evolution during a long ionic sputtering; (c) final result after long ionic sputtering.

The almost constant intensities of the niobium and oxygen peaks, after carbon is extinguished, clearly indicate the existence of an oxide-coated layer covering the surface of the sample, which does not corroborate the conclusions of Williams *et al.* (*32*) or Feng and Chen (*33*). As a matter of fact, the latter pointed out a very high stability of the surface level for natural molybdenite samples. Thus, our results show that $NbSe_2$ is much less steady than natural molybdenite in ambient air.

For a better fit between oxygen and niobium than that between niobium and selenium (the differences in electronegativity, as expressed on the Pauling scale, are respectively $\Delta x = 1.80$ for a Nb–O bond and $\Delta x = 0.91$ for a Nb–Se one), we must allow an oxide coating of niobium on the superficial layer. In contrast to iron, for which a composition gradient has been observed (*34*), this coating seems homogeneous. However, it is clear that such an oxide cannot be stoichiometric. The reason for this discrepancy is that such an altered film is thicker than 50 nm, considering the sputtering duration.

The evolution of the nitrogen peak during the experiment (increasing, then steady) indicates that this element is probably included in the empty sites situated between $NbSe_2$ sheets. Without other information, we can suppose that this element is sandwiched under dinitrogen molecules.

IV. Annealing Effect

An ambient air analysis having shown that the superficial composition is fairly different from that of the bulk sample, we studied the effects of a thermal treatment on the three kinds of samples previously obtained.

4.1. Cleaved Samples

To start with a clean surface, a cleaved $NbSe_2$ sample was surface sputtered in order to get rid of any adsorbed carbon deposits. Then its behavior was carefully observed under sputtering during a 30-min step

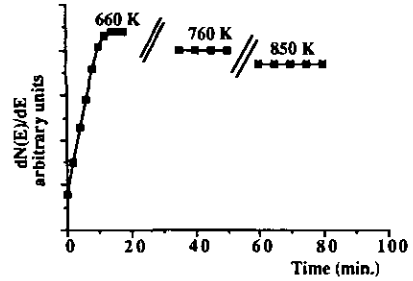

FIG. 4. Carbon segregation vs annealing duration.

heating at temperatures of 660, 760, and finally 850 K.

4.1.1. Carbon segregation. The evolution of the carbon peak vs annealing duration, which is represented in Fig. 4, points out a superficial segregation of that element at 660 K. Later thermal treatments, at 760 and 850 K, do not notably alter the height of the top level segregation point of the carbon peak.

However, it is difficult to determine the highest quantity of segregated carbon. As a matter of fact, this quantity is lower than those needed to obtain a carbon monolayer (atomic density is then $n \leq 10^{19}$ atom · m^{-2}). Therefore, this result shows that the volume of the melted product is very tiny (only a few ppm).

4.1.2. Variation of the superficial composition. The evolution of the peaks for carbon (272 eV), niobium (24 and 167 eV), and selenium (43 and 1315 eV), during the thermal experiments at 660, 760, and 850 K is represented in Fig. 5. At T = 850 K, all the peaks are about 10% lower, a phenomenon which has already been pointed out for Auger gain at high temperature with a similar device (*35*). Under those conditions, the decreases in the niobium and selenium peaks during the first heating at 660 K indicate segregation of carbon as described above. The resulting decrease in the signals is in the 20% range.

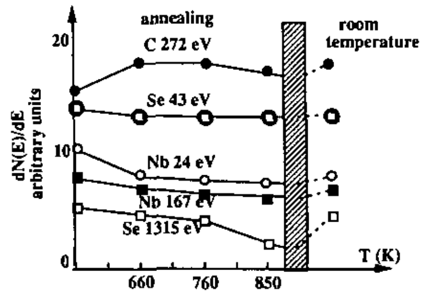

FIG. 5. Evolution of Auger signals during a high-temperature treatment.

The two selenium peaks correspond to quite different Auger electron escape depths, which are of 2 layers for the first peak (43 eV) and as deep as 15 for the second peak (1315 eV). The decrease in both signals observed at the beginning of sputtering is probably related to an initial increase in the surface concentration of selenium compared with the bulk composition on the one hand and to a sputtering of this element on the other hand (*36*).

As a result, evolution of those two peaks is quite meaningful since beyond 800 K, the 1315-eV peak intensity suddenly decreases to just 20% of its previous value, while the low-energy peak remains steady. This indicates a lack of selenium in the very first layers of the material bound to a vaporization of this element, and more importantly, the temperature itself is high. This result must be viewed together with the detection, by NbSe$_2$ Bourdon manometer, of a lack of selenium as early as 600 K (*21*).

After slow cooling, the intensity range of the two peaks returns to approximately its previous value in ambient air, which makes it certain that the compound has been rehomogenized during the cooling. Nevertheless, stoichiometry discrepancies are insignificant.

4.2. Uncleaved Samples

Regardless of the conservation method (ambient air, iodine), the two above-mentioned properties (carbon segregation and selenium desorption) may be found. This means the dissolved carbon concentration is always of a very small volume, thereby making Auger analysis possible, in contradiction with other investigations (*29*).

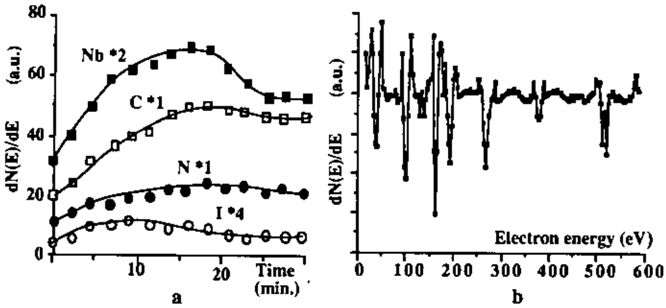

FIG. 6. Evolution of Auger signals during annealing at 400 K: (a) segregation of iodine; (b) the final result after long annealing.

The sample which could be examined immediately after being removed from the transport cell revealed some iodine and nitrogen adsorbed on the surface. After sputtering (Fig. 3c), the sample was taken to 400 K, and the evolution of the various peaks during heating is given in Fig. 6a. During the treatment an increase in the carbon, iodine, and niobium peaks can be noted as described above. Thus, there is surface iodine adsorption linked with volume; several alternate sputterings and heatings then give weaker and weaker quantities of adsorbed iodine until it disappears completely.

This result, along with a lack of iodine in the samples left in ambient air, indicates that halogen is dissolved at very low concentrations in the empty prismatic sites localized between two neighbor sheets of the single crystal (Fig. 6b). Its presence in a solved state may, however, notably modify the properties of materials: during Auger analysis a surprising temperature increase in the sample has taken place (about 80 K instead of 50 K for the others) for a 2-hr experiment.

The iodine can be present in two forms: as molecular diiodine inserted between the layers or in substitution for selenium in the covalent network. The first possibility is strongly reduced by the fact that the inserted molecules generally must play the role of a Lewis base, a property which is not well known for this halide. The second idea can be supported by the evolution of the cell parameters between the powder form and the single crystal form.

There is no apparent variation in the **c** parameter, although it is very sensitive to the intralayer insertion. On the other hand, the **a** parameter increases in the single crystal. Because it depends first on the nonmetal interactions in the sheets, its evolution could result from the substitution of Se^{2-} ions by large I^- ions (R (Se^{2-}) = 191 pm; $R(I^-)$ = 216 pm). This latter argument quite matches the results of ESCA analysis (*5*), although we do not think that the composition of such iodo–selenides will be clearly defined.

This phenomenon, due to poor elimination of electron and ion beams, could be indicative of a strong retention of electric charges and may be explained by the fact that the material has lost its metallic characteristics and is now a semiconductor. This result would thus explain why $NbSe_2$ crystals produce photoconversion of energy, by a photogalvanic effect, with a photocurrent gain 3 or 4 times higher than that obtained for powder samples (*12*).

V. Conclusions

The results of Auger spectroscopic analysis of $NbSe_2$ samples let us consider two physical phenomena: superficial reactivity and the effect of temperature on the surface.

A superficial characterization of $NbSe_2$ single crystals, grown by CVT with iodine as a transport agent, shows the great purity of their bulk (purity in volume) and the important reactivity of their surface. The latter is indicated by

1. A systematic contamination of the surface by carbon monoxide adsorption, even under an ultravacuum atmosphere.
2. The formation of a rather thick (probably more than 50 nm) air-altered oxide film, and nitrogen intercalation into the empty sites of the network, called Van der Waals' vacancies, with such a dissolution occurring after a long exposure of the sample to ambient air.
3. Superficial adsorption of iodine and nitrogen, after manufacturing.

Using Auger spectroscopy, Balchin observed similar behavior for $TiSe_2$ iodine transport (*31*). The evolution of the composition as far as 10 nm from the surface due to the fast air oxide coating of the material was noticed without any visible alteration of the sample and with only some tiny iodine deposits on the surface. Moreover, Mac Govern and Williams, using Auger analysis, pointed out an important pollution by carbon of natural molybdenite (*37*), which is favored by the presence of some defects.

A study of the influence of thermal treatments on the superficial composition of $NbSe_2$ made a complete analysis possible:

1. The carbon superficial segregation seen on the surface of the material indicates that there is some dissolved carbon in the bulk. The segregated quantity reaches a maximum value, which is found in any case without being precisely measured. It is less important than an adsorption single layer.
2. Selenium diminishes in superficial layers during heating, because of the migration of this element toward the surface and its vaporization. This proves that, beyond 720 K, this dichalcogenide is not thermally steady, which corroborates our observations by Bourdon manometer.
3. Superficial iodine and nitrogen adsorption during annealing shows there was a *dissolution* inside the material before these two elements were set up at empty sites of the crystalline network between $NbSe_2$ sheets or at empty selenium sites for iodine. The presence of dissolved iodine seems to give $NbSe_2$ a semiconductor character, thus confirming our photoconversion results with some $NbSe_2$ single crystals.

In conclusion, this original study (material synthesis and single crystal growth made under perfectly controlled conditions), coupled with AES analysis, leads to new results concerning not only niobium diselenide but also other transition dichalcogenides with lamellar structures. In the same way, it may be expected that, for other single crystals, $MoSe_2$ for instance, produced under the same conditions, some of the above results will be confirmed: purity within the material and presence of halogen (linked with the selected growth method) which may improve photoconversion yield (*9*).

Acknowledgment

This work has been supported by the French Space Agency, the Centre National d'Etudes Spatiales (CNES).

References

1. J. A. Wilson and A. D. Yoffe, *Adv. Phys.* **18**, 193 (1969).
2. L. H. Brixner, *J. Inorg. Nucl. Chem.* **24**, 257 (1962).
3. F. R. Gamble, J. H. Osiecki, and F. J. Di Salvo, *J. Chem. Phys.* **55**, 3525 (1971).
4. W. Bronger, *in* "Crystallography and Crystal Chemistry of Materials with Layered Structures" (F. Levy, Ed.), p. 93, Dordrecht (1976).
5. N. E. Lewis, T. E. Leinhardt, and J. G. Dillard, *Mater. Res. Bull.* **10**, 967 (1975).
6. H. Tributsch, *Z. Naturforsch. A* **32**, 972 (1977).
7. H. Tributsch, H. Gerischer, C. Clemen, and E. Buche, *Ber. Bunsenges. Phys. Chem.* **83**, 655 (1979).
8. N. D'Oliveira, O. Monnereau, G. Vacquier, O. Cerclier, and A. Casalot, *Ann. Chim. (Paris)* **7**, 651 (1982).
9. J. B. Legma, C. Vacquier, H. Traoré, and A. Casalot, *Mater. Sci. Eng B* **8**, 167 (1991).
10. S. Badrinarayanan, A. B. Mandale, and S. K. Date, *J. Electron Spectrosc. Relat. Phenom.* **34**, 79 (1984).

11. G. Vacquier, A. Rolland, and A. Casalot, *Mater. Sci. Eng. B* **85,** L9 (1987).

12. A. Casalot, M. Chaouch, and G. Vacquier, *Ann. Chim. (Paris)* **11,** 509 (1986).

13. J. B. Legma, G. Vacquier, and A. Casalot, *J. Cryst. Growth,* **130,** 253 (1993).

14. R. M. Lieth and J. C. Terhell, *in* "Preparation and Crystal Growth of Materials with Layered Structures" (R. M. Lieth, Ed.), p. 141, Reidel, Dordrecht (1977).

15. H. Schäfer, "Chemical Transport Reactions," Academic Press, New York (1964).

16. R. Nitsche, *Fortschr. Mineral.* **44,** 231 (1967).

17. G. Vachier, O. Cerclier, A. Casalot, R. Mamy, A. Couget, and F. Pradal, *Ann. Chim. (Paris)* **3,** 107 (1978).

18. R. Späh, U. Elrod, M. Lux-Steiner, E. Bucher, and S. Wagner, *Appl. Phys. Lett.* **43,** 79 (1983).

19. J. Omaly, M. Robert, and R. Cadoret, *Mater. Res. Bull.* **16,** 785 (1981) and **16,** 1261 (1981).

20. J. C. Launay, Thèse de Doctorat d'Etat, Univ. Bordeaux I. Bordeaux (1977).

21. G. Vacquier and A. Casalot, *Ann. Chim.* **18,** 1 (1993).

22. G. Vacquier and A. Casalot, *J. Cryst. Growth* **130,** 259 (1993).

23. A. Meerschaut and J. Rouxel, *J. Less-Common Met.* **39,** 1971 (1975).

24. A. Rolland and B. Aufray, *Surf. Sci.* **162,** 530 (1985).

25. A. Rolland, Thèse de Doctorat d'Etat, Univ. Aix-Marseille-III, Marseille (1982).

26. L. E. Davis, N. C. Mac Donald, P. W. Palmberg, G. E. Riach, and R. E. Weber, "Handbook of Auger Electron Spectroscopy," Phys. Electron. Ind. Inc. Publ., MN (1976).

27. B. J. Mrstik, R. Kaplan, T. L. Reinecke, M. Van Hove, and S. Y. Tong, *Phys. Rev. B* **15**(2), 897 (1977).

28. F. F. Abraham and C. R. Brundle, *J. Vac. Sci. Technol.* **18,** 506 (1981).

29. G. Allie, R. Baudoing, E. Blanc, and Y. Gauthier, *in* "Proceedings of the Surface Vide and Metallurgy European Symposium," p. 353, *Vide* (special issue) (1978).

30. P. Molinié, Thèse de Doctorat d'Etat, Univ. Nantes, Nantes (1977).

31. A. A. Balchin, *J. Mater. Sci. Lett.* **2,** 457 (1983).

32. R. H. Williams, I. G. Higginbotham, and M. A. Whitaker, *J. Phys. Chem. Solids* **5,** L191 (1972).

33. H. C. Feng and J. M. Chen, *J. Phys. Chem. Solids* **7,** L75 (1974).

34. A. Rolland, unpublished work.

35. A. Rolland, J. Bernardini, and M. G. Barthes-Labrousse, *Surf. Sci.* **143,** 579 (1984).

36. P. S. Ho, *Surf. Sci.* **72,** 253 (1978).

37. I. T. Mac Govern and R. H. Williams, *Surf. Sci.* **46,** 427 (1974).